Virtual Cells for Infrastructureless MANETs

Salman Al-Shehri and Pavel Loskot
College of Engineering
Swansea University
Swansea, United Kingdom
{609122,p.loskot}@swan.ac.uk

Tolga Numanoğlu and Mehmet Mert
ASELSAN A.S.
Communications and IT Division
Ankara, Turkey
{tnumanoglu,mmert}@aselsan.com.tr

***Abstract*—Mobile ad-hoc networks (MANETs) are deployed and operate in infrastructure-less environments. However, when the nodes in such networks are aware of their locations, a shared grid of virtual cells can be defined. It is then possible to pre-assign these cells with communication channels and other radio resources to facilitate distributed radio resource management (RRM) and to limit the exchange of control messages. The channel allocations in virtual cells can assume similar channel reuse schemes as those used in the legacy cellular networks. Assuming that the node clusters coincide with the virtual cells, the average signal-to-interference-noise ratio (SINR) is numerically compared for a random waypoint mobility (RWM) model with a deterministic component, and two sample designs of the orthogonal frequency hopping patterns assigned to the clusters of 3 and 7 virtual cells, respectively.**

I. Introduction

The legacy cellular networks exploit a base station architecture to provide uplink and downlink radio access for the wireless subscribers [1]. In many other scenarios it is impractical to plan and deploy the supporting network infrastructure, so the network topology is established by enabling direct device-to-device (D2D) communications [2]. The resulting ad-hoc or mesh topology of MANETs and VANETs supports mobility of the network nodes [3]. Such networks are used extensively for environment sensing (e.g., in agriculture), system monitoring (e.g., the Internet of Things and wireless sensor networks), and in military applications (e.g., tactical networks). However, they are facing many challenges such as adverse propagation conditions, battery, bandwidth and computing constraints as well as security issues.

The RRM in wireless networks includes allocating communication channels, and setting the transmitting powers and data rates in order to use the limited radio resources as efficiently as possible [1]. Unlike the cellular networks with centralized base station controllers, the RRM in MANETs is fully distributed, so the network nodes have to exchange enough information to coordinate multiple access, create network topology, manage interference, and determine routing [4]. The scalability of practical ad-hoc networks is often achieved by a two-tier topology where the network nodes are organized in clusters which are controlled by their respective cluster-heads [5]. The nodes in a cluster are usually one or two hops away from their cluster head. The cluster heads centrally allocate radio resources within their cluster, however, the allocation of radio resources among the clusters remains distributed.

Virtualization of the radio resources has recently emerged as a new paradigm to provide flexibility in efficiently sharing the network physical infrastructure among the heterogeneous users [6]. The network physical resources are aggregated into a network cloud, and then optimally partitioned to match the current demand of different network users. This enables to define virtual network functions (NFV), virtual radio access networks (V-RAN), virtual operators and so on. Virtualization is also expected to be a key component in the upcoming 5G networks [7]. On the other hand, virtualization of the distributed radio resources in infrastructure-less networks is much more difficult, so it is rarely considered in literature [8].

In this paper, we consider a novel virtualization strategy for MANETs. It assumes that all network nodes are aware of their own geographical location. The nodes a priory agree a set of geographically distributed reference points referred to as the anchors. The virtual cells are then the Voronoi regions of these anchor points in a 2D plane. Hence, the nodes can readily determine in which virtual cell they are located. Each virtual cell is pre-assigned default radio resources which can greatly simplify the distributed RRM. In particular, the virtual cells can facilitate creation of clusters, and the interference management by defining orthogonal communication channels among the cells. More importantly, various mappings between the network clusters and the virtual cells can be devised to match the specific mobility models encountered.

The location information is provided by the Global Navigation Satellite System (GNSS) receivers [9]. In military tactical networks, the GNSS signal may be subject to jamming. The timing information provided by the GNSS can be used to achieve time synchronization among the network nodes [10]. We illustrate the main idea of virtual cells in MANETs assuming narrowband transmissions with frequency hopping, and time-division and frequency-division multiple access (TDMA and FDMA). Other relevant concepts which are, however, outside the scope of this paper are: relative mutual localization of the network nodes (e.g., using triangulation) to establish virtual cells, fractional and soft frequency reuse (FFF and SFR) to trade-off the cell capacity with coverage [11], the location predictive RRM [12], and the geographical routing [13]. The trajectory extrapolations are exploited to improve the connectivity of MANETs in [14].

II. System Model

A wireless network consisting of N nodes is deployed in a 2D geographical area $\tilde{\mathcal{G}}$. The i-th node coordinates $\boldsymbol{z}_i(t) \in \tilde{\mathcal{G}}$ at time t are given by a random mobility model of that node. The expected node trajectory,

$$\mathrm{E}[\boldsymbol{z}_i(t)] = \bar{\boldsymbol{z}}_i(t)$$

is deterministic, but time-varying, while the variations of the node trajectory can be measured as,

$$\mathrm{var}[\boldsymbol{z}_i(t)] = \mathrm{E}\Big[\|\boldsymbol{z}_i(t) - \bar{\boldsymbol{z}}_i(t)\|^2\Big]$$

where $\|\cdot\|$ is the Euclidean norm. In the reference point group mobility (RPGM) model [15], the mean trajectory $\bar{\boldsymbol{z}}_i(t)$ is the same for the nodes in a group, for example, for the nodes in the same cluster. Since the mean trajectory is known beforehand (i.e., deterministic), it can be sampled at discrete time instants $t_1, t_2, \ldots, t_j, \ldots$ to pre-define the anchor points $\boldsymbol{a}_i[j]$ before the network is deployed. In such case, we can define,

$$\boldsymbol{a}_i[j] = \bar{\boldsymbol{z}}_i(t)\big|_{t=t_j}.$$

More importantly, the location of anchor points $\boldsymbol{a}_i[j]$ can be optimized for a given initial distribution of nodes and their mobility. In particular, a large number of anchor points yield smaller virtual cells and more frequent handovers between them as the nodes move around. On the other hand, the virtual cells with large area may contain too many nodes, so the benefits of separating nodes into virtual cells diminish. For simplicity, in this paper, we determine the conditions when the optimum virtual cells are given by the standard hexagonal layout of the legacy cellular networks.

Assume the time-derivative of the mean trajectories of all nodes is the same, i.e., let,

$$\frac{\mathrm{d}}{\mathrm{d}t}\bar{\boldsymbol{z}}_i(t) = \bar{\boldsymbol{v}} \;\forall i$$

where $\boldsymbol{v}$ is a common speed vector, i.e., the mean trajectories of all nodes are parallel to each other. Provided that the random component of the node trajectories, $\boldsymbol{z}_i(t) - \bar{\boldsymbol{z}}_i(t)$, is uniformly distributed in all directions, it follows the RWM model [15]. In this case, the optimum anchor points lie on a rectangular grid with dimensions $\sqrt{3}R/2$ and $3R/2$, respectively, where $R > 0$ is a scaling factor. The value of R is set to match the initial locations of the nodes and the mobility variance $\mathrm{var}[\boldsymbol{z}_i(t)]$, for example, to evenly distribute the nodes among the virtual cells. The anchor grid is rotated, so that it is aligned with the mean speed vector $\bar{\boldsymbol{v}}$. The hexagonal cells are then the Voronoi regions of the anchor points with the 2D coordinates,

$$\boldsymbol{a}_{m,n} = \left[R m \bmod_2 (n-1),\; R\frac{\sqrt{3}}{2} n\right] \tag{1}$$

for all integers m and n where R now represents the outer radius of the virtual cells. The list of anchor points can be stored in every node before their deployment. The nodes determine their location in the particular virtual cell by finding the nearest anchor point. Furthermore, the virtual cells can be sectored to aid the RRM as explained below.

A. Radiowave Propagation

Every node employs a single omni-directional antenna. The radio transmissions are subject to fading and path-loss propagation conditions [11]. The signal channel attenuation may represent both fading and shadowing. For simplicity, the fading coefficients h are assumed to be independent and Rayleigh distributed with the same variance. The path-loss at distance d from the transmitter is modeled as,

$$\Gamma(d) = \Gamma_0 \times d^{-\mu}$$

where $\mu > 1$ is the path-loss coefficient. Assuming the free-space path-loss, the attenuation factor, $\Gamma_0 = \lambda_c/(4\pi)$, and $\mu = 2$, where λ_c is the carrier wavelength.

The nodes are capable of full duplex transmissions provided that they transmit and receive at different frequency channels. The nodes can either transmit or listen at multiple frequency channels at once, i.e., the transmitted signals are a sum,

$$s(t) = \mathrm{Re}\left\{\sum_i \hat{s}_i(t)\, \mathrm{e}^{\mathrm{j}2\pi f_i t}\right\}$$

of the modulated signals $\hat{s}_i(t)$ at the carrier frequencies,

$$f_i = f_\mathrm{c} + \Delta f_i.$$

The received signal strength (RSS) at node j listening in a given time-frequency slot for the intended transmission from another node i can be written as [11],

$$\mathrm{RSS}_j = P_i h_{ij} \Gamma(d_{ij}) + W_0 + \sum_{i \neq j} P_i h_{ij} \Gamma(d_{ij})$$

where d_{ij} is the distance between nodes i and j, W_0 is the power spectral density (PSD) of the background noise, and the last sum corresponds to the co-channel interference. We assume a simple truncated power control mechanism, so the transmit power P_i of the node i is set as,

$$P_i = \min(1/\Gamma(d_{ij}), P_\mathrm{max}) \tag{2}$$

where P_max is the maximum available or allowed transmit power which is the same for all nodes. Note that the policy (2) binds the transmit power to the distance of the target node j. Provided that the value P_max is sufficiently large, the policy (2) effectively removes the path-loss between many pairs of nodes, so their geographical separation becomes irrelevant.

The key metric to evaluate the radio resource allocation schemes with virtual cells in MANETs is the SINR. For node j receiving at some time-frequency channel, it is defined as,

$$\begin{aligned}\mathrm{SINR}_j &= \frac{P_i h_{ij} \Gamma(d_{ij})}{\mathrm{RSS}_j - P_i h_{ij} \Gamma(d_{ij})} \\ &= \frac{P_i h_{ij} \Gamma(d_{ij})}{W_0 + \sum_{i \neq j} P_i h_{ij} \Gamma(d_{ij})}\end{aligned}$$

where the PSD W_0 can be determined to set a desired signal-to-noise ratio (SNR) as,

$$W_0 = P_\mathrm{max}/\mathrm{SNR}.$$

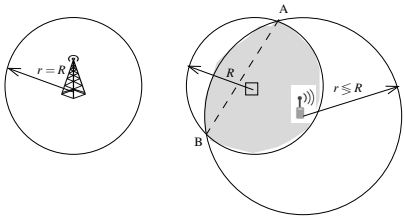

Figure 1. The legacy cell coverage (left), and the virtual cell coverage (right). The square node represents the anchor point of the virtual cell.

III. Radio Resources Allocation

As in the legacy cellular networks, the frequency channels can be reused in different virtual cells to increase the overall system capacity. The reuse distance for the hexagonal virtual cells defined by the anchor locations (1) is calculated as [1],

$$d_{\text{reuse}} = R\sqrt{3N_{\text{cl}}}$$

where $N_{\text{cl}} = (u^2 + v^2 + uv)$ is the number of cells in the cell cluster, and u and v are the number of cells which are crossed to arrive to the nearest co-channel cell within the hexagonal grid. Typical values of N_{cl} are $1, 3, 4, 7$ and 9. In general, the larger the ratio d_{reuse}/R, the better the isolation between the reused frequency channels, and the better the SINR. However, the cell coverage between the legacy and the proposed virtual cellular system differs as shown in Fig. 1. In the former, the base station is at the cell center, so the cell radius R and the base station transmission range r are equal. In the latter, the transmission range r of the node at the virtual cell edge would have to be at least $r \geq 2R$ to cover the whole cell area. The shaded area in Fig. 1 which is covered by the wireless node can be calculated as [16]:

$$A_{\text{coverage}} = \begin{cases} ccA(r,d_1) + A(R,d_2) & d_{12} = d_1 + d_2 \\ A(r,d_1) + \pi R^2 - A(R,d_2) & r > d_{12} \end{cases}$$

where d_1 and d_2 are the distances to the anchor point and to the wireless node from the line A-B, respectively, and d_{12} is the distance between the wireless node and the anchor point.

Assume there are F orthogonal frequency channels defined within the total bandwidth allocated to the network. Let F/N_{cl} be an integer, so the channels can be divided equally among the virtual cells in the same cell cluster. Some radios such as those used in military tactical networks use encrypted frequency hopping schemes to create a resilience against the jamming [5]. In this case, the virtual cells in the same cell cluster can be allocated a set of orthogonal time-frequency hopping patterns. However, these hopping patterns are only orthogonal as long as all transmissions are time slot synchronized. Since the neighboring cells within the same cell cluster may not be time synchronized, we can reduce the resulting co-channel interference by requiring that every frequency channel is used within the cell cluster only once every $X > 0$ consecutive time slots. In particular, assuming $X = 3$, the channel allocation matrix $\boldsymbol{F}$ is resilient against the time-slot misalignment of the neighboring transmissions by up to one time slot. The following Matlab code generates the orthogonal channel allocation matrix $\boldsymbol{F}$ of $X \times N_{\text{cl}}$ frequency tones over T consecutive time slots for N_{cl} cells in the cell cluster. The resilience property of the channel allocation matrix $\boldsymbol{F}$ will be shown numerically in the subsequent section.

Algorithm to generate frequency hopping matrix $\boldsymbol{F}$

```
% randint(K) generates random integer
% between 1 and K
NA= zeros(3*Ncl,T); % aux matrix
FF= zeros(Ncl,T);   % channel matrix
for u=1:Ncl
  for t=1:T
      i= find(NA(:,t)==0);
      j= randint(length(i));
      FF(u,t)= i(j);
      NA(i(j),t)= 1;
      if t==T, t1=1; else t1=t+1; end
      NA(i(j),t1)= 1;
      if t==1, t1=T; else t1=t-1; end
      NA(i(j),t1)= 1;
  end
end
```

IV. Transmission Protocols

Note that it is important to distinguish between the node clusters defined among the network nodes, and the cell clusters defined for the frequency channel reuse among the virtual cells. Employing proprietary protocols instead of the legacy TCP/IP based protocols leads to improved utilization of the radio resources in MANETs [4]. However, the protocol development and optimization is a very complex matter, and certainly beyond the focus of this paper. Here, we only discuss layer 2 protocols for the proposed virtual cells in MANETs. We assume a two-tier network topology where the nodes are grouped in node clusters, so the packets are routed within and among the clusters. Each cluster is assigned a single cluster head node. The nodes connected to more than one cluster head serve as the gateway nodes between the node clusters. The nodes can play other roles such as relaying the packets for other nodes as well as creating traffic flows by generating and consuming the packets. We assume that each virtual cell is assigned a single frequency channel or a set of frequency hopping patterns. The node transmissions follow these rules:

1) The nodes in a given virtual cell can transmit only using the frequency channel or the frequency hopping pattern assigned to that cell. However, the nodes can listen to transmissions at multiple frequencies assigned to other neighboring cells.
2) The nodes within a given virtual cell use TDMA or mutually orthogonal frequency hopping patterns.
3) The nodes in different cells of the virtual cell cluster use FDMA or the assigned frequency hopping patterns.

In general, the network clusters can be created independently of the nodes locations within the virtual cells [17]. Consequently, the virtual cells can contain nodes belonging to different node clusters, or there may be no cluster head within

the virtual cell to time-synchronize the nodes and make their transmissions orthogonal. In order to overcome these issues and create the node clusters within the virtual cells, we assume the following assignment of the node roles in the virtual cells:

1) The nodes located within the same virtual cell form a single cluster.
2) The node closest to the anchor point (i.e., the cell center) of the virtual cell becomes the cluster head.
3) The nodes at the edge of the virtual cell are consider to become the gateway nodes for the node cluster.

Choosing the cluster head close to the cell center leads to more efficient coverage of the cell, and smaller transmission distances from other less centered nodes. The gateway nodes are selected to be close to the cell edge, and at the same time, they should be in different angular sectors. Since the packet relaying increases the number of transmissions (as well as the number of hops) in the cell, it should be limited. The role assignment to the nodes can be done by modifying the existing protocols which are used for creating the node clusters [17]. Splitting of the virtual cells can be used to selectively poll the nodes in a predetermined order, for instance, the polling message requests a response from the nodes in a given cell sector. The node roles are periodically updated as they move around. The node handover when leaving one cell and joining another cell can be performed by contacting the cluster head in the new cell and requesting the allocation of radio resources in that new cell. The RRM performed by the cluster heads can be aided by exchange of the location information among the nodes in the same virtual cell.

V. Numerical Examples

Numerical experiments were performed in order to evaluate the co-channel interference and the corresponding SINR achievable in the virtual cellular MANETs. The anchor points are regularly distributed according to (1), assuming the cell radius $R = 500$m. There are $N = 200$ nodes initially uniformly distributed in a movable observation rectangular area of $2,500\text{m} \times 2,500\text{m}$. The deterministic component of the node movements is exactly horizontal whereas the random mobility component assumes the RWM model. The nodes are moved and their roles reestablished once every time slot.

We assume the following transmission protocol. There is exactly one cluster-head in each virtual cell, and it is the node closest to the anchor point (i.e., the virtual cell center). Each cell is also allocated up to 3 gateway nodes. In particular, the gateways are the nodes furthest away from the cell center in each of the 3 sectors: 30° to 150°, 150° to 270°, and -90° to 30°, respectively. Hence, it is possible that, in some virtual cells, the cluster-head also acts as a gateway to transmit packets to the neighboring cells, otherwise, the cluster-head transmits packets to the nodes within the same cell. The remaining nodes in the virtual cells only retransmit packets to the other nodes within the same cell. The pairs of transmitting and receiving nodes in the virtual cells are generated at random with a uniform probability. The pairs are selected independently from one time slot to another as well as independently among the different cells. Thus, all transmissions within the same cell are orthogonal unlike the simultaneous transmissions in different cells. Furthermore, the transmissions assume frequency hopping where every cluster of the virtual cells is assigned a distinctive set of mutually orthogonal frequency hopping patterns. These patterns are generated by the algorithm presented in Section III. Even though the transmissions in each cell at every time slot are orthogonal, the co-channel interference can still appear due to a lack of time-slot synchronization among the virtual cells, even within the same cell cluster. We assume the virtual cell clusters with $N_{\text{cl}} = 7$ and $N_{\text{cl}} = 3$ cells (equal to the frequency reuse factor) shown in Fig. 2 and Fig. 3, respectively. The arrows in these figures indicate randomly chosen transmissions in a given time slot. There is either one or two orthogonal transmissions per cell in each time slot. We consider the following 4 transmission schemes to compare.

The first scheme, denoted as FR=7/2x7, uses $2 \times 7 = 14$ distinct and orthogonal frequency channels with 2 of these channels allocated to each cell in the cluster of $N_{\text{cl}} = 7$ cells. Hence, there can be up to 2 simultaneous orthogonal transmissions in each cell in any given time slot. The frequency hopping pattern is created by randomly selecting 2 of the allocated frequency channels during every time slot. The second scheme, denoted as FR=7/1x7, assumes 7 orthogonal frequency hopping patterns over $3 \times N_{\text{cl}} = 21$ frequencies; one such pattern is allocated to each cell in the cell cluster. An example of these patterns generated by the algorithm from Section III is given in Table I. The third scheme, denoted as FR=3/2x3, uses $2 \times 3 = 6$ distinct and orthogonal frequency channels the same way as the first scheme, but assuming only $N_{\text{cl}} = 3$ cells in the cell cluster. The fourth scheme, denoted as FR=3/1x3, assumes 3 orthogonal frequency hopping patterns over $3 \times N_{\text{cl}} = 9$ frequencies which are generated and used the same way as in the second scheme.

The simulation results for $T = 100$ time slots are shown in Fig. 4, Fig. 5 and Fig. 6. The simulations were performed in Matlab. In particular, Fig. 4 investigates the dependency of the average SINR on the SNR for the four schemes described above, and assuming the maximum transmission power set to $P_{\text{max}} = 20$W. As expected, the 7-cell cluster with only one transmission per cell in each time slot experiences the smallest amount of the co-channel interference. The difference between 3-cell and 7-cell clustering is significant, especially at larger values of SNR. Fig. 5 shows the dependency of the average SINR on the maximum transmission power of nodes P_{max} for the fixed SNR of 20dB. In the simulations, we observed that there exist a power threshold when the average SINR suddenly decreases. Thus, limiting the transmission powers appears to also limit the co-channel interference. However, more investigations are needed to better understand this phenomenon.

Finally, the impact of time synchronization on the level of co-channel interference can be seen in Fig. 6. Unlike Fig. 4 and Fig. 5 where the transmissions are assumed to be perfectly time-slot synchronized, here, we assume that the transmissions at the neighboring cells can be misaligned by up to one time-

slot corresponding to $\Delta T = 100\%$. Thus, given the value of ΔT, the transmissions in $(N_{\text{cl}} - 1)$ neighboring cells are delayed by a fixed but randomly chosen time from the interval $(0, \Delta T)$. We observe that the frequency hopping patterns generated by the algorithm from Section III are constrained such that the time delays by up to one time slot do not create any additional co-channel interference. On the other hand, the schemes FR=7/2x7 and FR=3/2x3 generate additional co-channel interference if the transmissions at subsequent time slots at neighboring cells are occurring at the same frequency.

VI. Discussion and Conclusions

The GNSS localization consumes additional energy, however, it is routinely available at the nodes in tactical and sensor networks operating in the outdoor environments. The geographical partitioning of the area using a set of predetermined locations referred to as the anchor points and the corresponding Voronoi regions can facilitate the frequency, or more generally, channel planning. The reuse and assignment of communication channels in the cells is one of the main tasks of the base station controllers in the legacy cellular networks. Here, this task is accomplished without any supporting physical infrastructure, so the MANETs can take advantage of the virtually defined cells. The infrastructureless virtual cells should be contrasted from the NFV and other virtualization strategies which are used to pool and partition the shared radio resources in the radio access networks.

In this paper, we adopted several simplifying assumptions to illustrate the proposed concept of virtual cells in MANETs. In particular, the deterministic component of the node mobility is parallel for all nodes, and have the same magnitude, although the cell handovers, and reassignment of the node roles has been performed. Our simulations are only concerned with the multiple access (layer 2) protocols. The routing would affect the transmission scheduling and the network congestion. We investigated the transmission rules where the nodes can only transmit in the channels preassigned to the virtual cells whereas there was otherwise no restriction to which channels the nodes can listen to. We did not consider how the nodes can further exploit sharing their location information other than in determining their roles within the virtual cells.

Much more sophisticated patterns of the anchor points could be devised. As explained in Section II, the hexagonal regular cells are only optimum for very specific mobility model considered in this paper. Defining the optimum anchor points for general mobility models is an open research problem. Furthermore, the cluster heads in each virtual cell can adaptively request additional radio resources from the neighboring cells, provided that their cell contains too many nodes. This RRM strategy would better match the spatial node distribution in the virtual cells. More importantly, the node clusters may not be contained within single virtual cells as considered in our simulations. In this case, a cluster head may be managing multiple virtual cells, or a virtual cell may be managed by multiple cluster heads. Another interesting problem is to investigate the co-existence of multiple MANETs with defined virtual cells, or the case of overlay virtual cellular networks. The interference due to asynchronous transmissions could be mitigated by the use of spread-spectrum and multi-antenna systems.

In summary, we observed that the transmission schemes considered are significantly affected by the assumed power control mechanism, i.e., restricting the transmitting powers generates less co-channel interference. We designed the frequency hopping patterns that are robust against time-slot misalignment between the neighboring virtual cells, although such patterns require larger number of frequency slots than the simple non-orthogonal frequency hopping patterns. Our findings reported in this paper indicate that the concept of virtual cells is a promising approach for use in tactical networks and other types of MANETs with ad-hoc topology, whether these networks assume node mobility or not.

References

[1] K. Pahlavan and A. H. Levesque, *Wireless Information Networks*. John Wiley, New Jersey, 2005.

[2] C. K. Toh, *Ad Hoc Mobile Wireless Networks: Protocols and Systems*. Prentice Hall, 2002.

[3] M. Mauve, J. Widmer, and H. Hartenstein, "A survey on position-based routing in mobile ad hoc networks," *IEEE Network*, vol. 15, no. 6, pp. 30–39, Nov. 2001.

[4] B. Karaoglu, B. Tavli, T. Numanoglu, and W. Heinzelman, *Energy Efficient Real-Time Distributed Communication Architectures for Military Tactical Comm. Systems*. IGI Global, 2015, ch. Chapter 2, pp. 35–82.

[5] L. Y. Cheung and C. W. Ying, "Designing tactical networks - perspectives from a practitioner," Jun. 2013, dSTA Horizons, Tech. Rep.

[6] S. Khatibi and L. M. Correia, "Modelling virtual radio resource management in full heterogeneous networks," *EURASIP J. Wireless Commun. Network.*, no. 73, pp. 1–17, Apr. 2017.

[7] ITU-R Rec., "IMT vision - framework and overall objectives of future development of IMT for 2020 and beyond," Sep. 2015, M.2083-0.

[8] A. Lehmann, A. P. Tchinda, and U. Trick, "Optimization of wireless disaster network through network virtualization," in *Prof. Int. Network Conf.*, 2016, pp. 165–170.

[9] H. Wymeersch, J. Lien, and M. Z. Win, "Cooperative localization in wireless networks," *Proc. IEEE*, vol. 97, no. 2, pp. 427–450, Feb. 2009.

[10] B. Sundararaman, U. Buy, and A. D. Kshemkalyani, "Clock synchronization for wireless sensor networks: a survey," *Ad Hoc Networks*, no. 3, pp. 281–323, 2005.

[11] T. D. Novlan, R. K. Ganti, A. Ghosh, and J. G. Andrews, "Analytical evaluation of fractional frequency reuse for OFDMA cellular networks," *IEEE Trans. Wireless Commun.*, vol. 10, no. 12, pp. 4294–4305, 2011.

[12] S. Rajagopal, N. Srinivasan, R. Narayan, and X. Petit, "GPS based predictive resource allocation in cellular networks," in *ICON*, 2002, pp. 229–234.

[13] A. Jadbabaie, "On geographic routing without location information," in *IEEE CDC*, vol. 5, 2004, pp. 4764–4769.

[14] L. L. Dai, "Proactive mobile wireless networks: An infrastructureless wireless network architecture for delay-sensitive applications," 2008, Massachusetts Instit. of Technology, PhD Thesis.

[15] G. Jayakumar and G. Ganapathi, "Reference point group mobility and random waypoint models in performance evaluation of MANET routing protocols," *J. Comp. Systems, Networks, and Comms.*, vol. 2008, no. 860364, pp. 1–10, 2008.

[16] E. W. Weisstein, "Circle-circle intersection," From MathWorld–A Wolfram Web Resource. Available: http://mathworld.wolfram.com/.

[17] R. Agarwal and M. Motwani, "Survey of clustering algorithms for MANET," *Int. J. Comp. Science and Eng.*, vol. 1, no. 2, pp. 98–104, 2009.

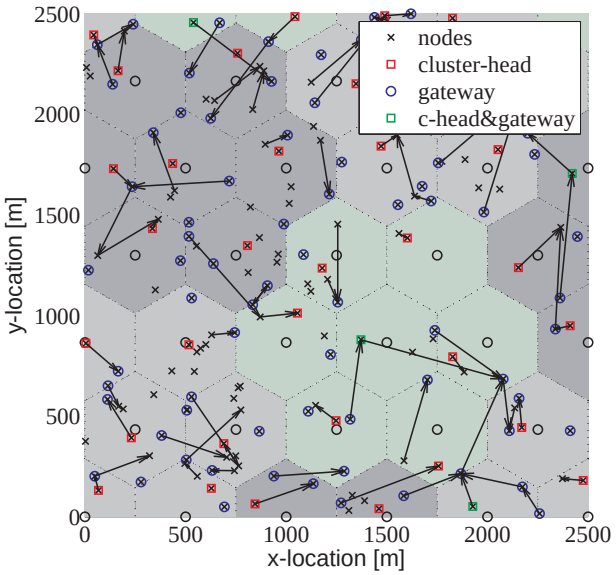

Figure 2. A snapshot of transmissions in the 7-cell cluster network.

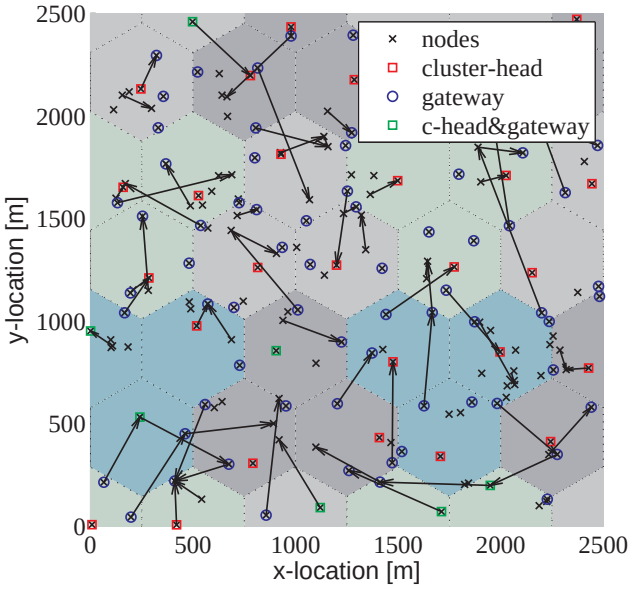

Figure 3. A snapshot of transmissions in the 3-cell cluster network.

Table I
A SAMPLE ORTHOGONAL ALLOCATION OF 21 CHANNELS TO A CLUSTER OF 7 CELLS OVER 10 TIME-SLOTS

Cell# 1	20	17	5	19	7	4	19	21	9	6
Cell# 2	18	10	8	11	5	18	5	13	17	14
Cell# 3	4	16	2	16	10	20	17	20	1	2
Cell# 4	11	12	15	1	13	8	12	15	4	3
Cell# 5	19	1	21	14	21	9	1	11	7	15
Cell# 6	5	3	18	3	6	15	14	6	12	8
Cell# 7	9	14	4	17	12	3	10	16	10	13

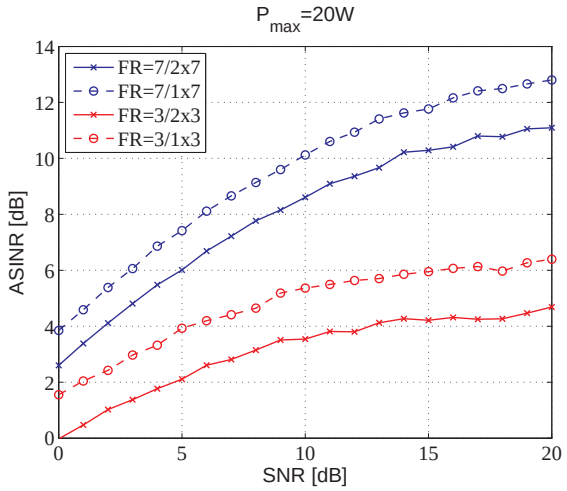

Figure 4. The average SINR versus SNR for 4 channel allocation schemes.

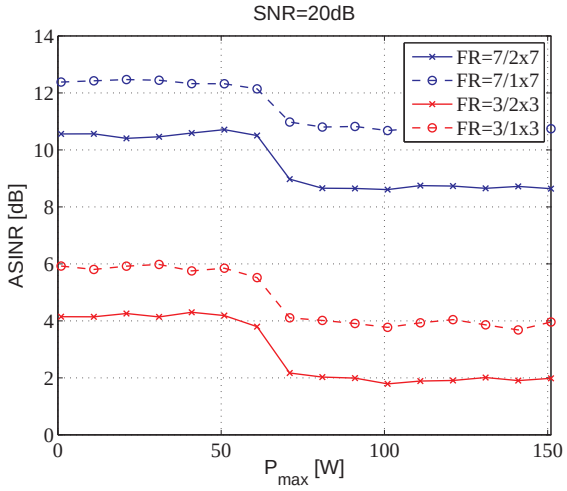

Figure 5. The average SINR versus the maximum transmit power $P_{\max}$ for 4 channel allocation schemes.

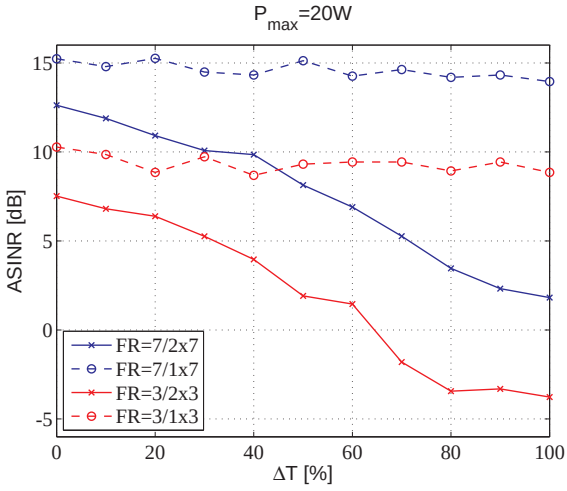

Figure 6. The average SINR versus the timing difference ΔT for 4 channel allocation schemes.